

## Development of Electrical Runout Online Measurement System Based on Eddy Current Technique and Laser Triangulation

<sup>1</sup>Wang Yifeng, <sup>2</sup>Cao Yanlong, <sup>2</sup>Chen Xiaolong, <sup>2</sup>Lin Zaiyu,  
<sup>2</sup>Yang Jiangxin

<sup>1</sup> School of Mechanical and Automotive Engineering, Zhejiang University of Science and Technology, Hangzhou, 310023, China

<sup>2</sup> Institute of Advanced Manufacturing Engineering, Zhejiang University, Hangzhou, 310027, China

<sup>2</sup> Tel.: 0571-87953198

<sup>2</sup> E-mail: sdcaoyl@zju.edu.cn

Received: 28 April 2013 /Accepted: 19 July 2013 /Published: 31 July 2013

**Abstract:** Material electromagnetic multidistribution of large rotors poses a potential hazard to the operation of rotary machine and interferes the vibration monitoring. These variations of electromagnetic property of material are scaled as electrical runout, which is necessary to be controlled in manufacturing process. A method of offsetting transducer difference for detecting electrical runout online is presented in this paper through finite element analysis, and the corresponding measurement system is developed for large air compressor rotors. A beam of laser with triangulation method is used to measure the surface position of the revolving rotor, which can be transformed as the non-contact distance. In the condition of static sensor probe, rotating centerline and rotary measured points on surface, actual runout of rotor is calculated through signal obtained from laser triangulation measurement. In this way, eddy current sensor, which is posed in the same plane of measuring cross profile with laser device, detects both actual runout and electrical runout as output of total indicated runout. Analyzing two signals through adjusting the phases of cross profile and offsetting the actual runout, electrical runout can be indicated in the process of lathe working. This measurement capability is useful in predicting the vibration level in the slow roll testing before product delivery. At last, the measuring experiment is performed to verify the accuracy of the system. Copyright © 2013 IFSA.

**Keywords:** Electrical runout (ERO), Eddy current sensor, Laser triangulation technique, Optical measurement system.

### 1. Introduction

Material electromagnetic uneven of large rotors called electrical runout poses a potential hazard to the running stability of rotary parts and interferes the vibration monitoring. The vibration limits resulted in the more common use of eddy current sensor probes to measure and monitor vibration of shaft. Electrical

runout and mechanical runout will appear to be vibration and result in measurement error [1]. The vibration reading can appear either too high or too low because of the error may incorrectly result in disassembly of the machine and re-work of the probe track area. Therefore, API standards has defined limits for the maximum runout, according to API612, the limit for slow roll runout is 25 % of the allowable peak-to-peak vibration amplitude or 0.25 mils [2].

The variation in properties of eddy current sensor depends on the interaction of the two magnetic fields. The impedance of coil is a function of lift-off, the excitation frequency, the conductivity and permeability of material. When measuring distance using eddy current sensor for non-stationary target, the variation of conductivity  $\sigma$  and permeability  $\mu$  of rotor material becomes the disturbance for detecting variation of lift-off which is so called electrical runout.

ERO problem of rotors with eddy current sensor and its measuring principle have drawn attentions of more and more researchers in recent years. For example, in 1976, Biggs [3] presented a patent to remove the ERO by redistributing the local electromagnetic properties of the shaft surface by cold work. They used means of a peening operation on the shaft to cold work the same. Tian et al [4, 5] analyzed the influences of some parameters, such as the resistivity of the target, the permeability in the target and converting circuits, on the sensor's output and the modulation ways for samples. In order to minimize the influence of the inhomogeneity, they increased the excitation coil frequency in AM sensors and oscillating frequency in FM sensors. Petar B. Petrovic et al [6] tried to solve ERO problem using signal processing, they presented an approach to compensate the electrical runout error dynamically based on discrete wavelet transform. Yu Yating et al [7, 8] investigated the contributions of material electromagnetic properties and lift-off on ERO signal, they found that the rational line of resistance and inductance is linear and parallel under different lift-off. Finally, they proposed a method of demagnetizing to remove electrical runout, the efficiency of which was indicated by a series of experiments. In the other side, the calculation and analysis of impedance is important for eddy current problem. In 1970s, Dodd et al initially presented closed form expressions for models analysis [9], and then, they used matrix method to extend the models to an arbitrary number of layers [10, 11]. Theodoros Theodoulidis et al [12] expanded the integral solution. As a result, both computation speed and accuracy control were optimized.

The finite element numerical method has been implied in computing impedance of coil in eddy current measurement successfully [13]. Ida N. et al [14] used the finite element method to design absolute and differential eddy current probes. Norton S. J. et al [15] using Maxwell's equation to inverse eddy current problem. However, Vyrubal D. et al [16] and Kim S. D. et al [17] indicated the above theory is unreliable by experiment. Tae-Ok Kim et al [18] developed a new modeling method to improve the accuracy of the eddy current sensor and solve the problem of calibration. In their method, the sensor coil and the eddy current's geometric was simplified into an array of circular loops. M'hemed Racheck et al [19] developed a three-dimensional numerical method to calculate the response of eddy current probes.

In this paper, the model of ERO measuring using eddy current sensor is built by FEM firstly, and the measuring method of ERO has been analyzed from the influences. Then the design of measuring system based on eddy current technique and laser triangulation is performed. Finally, the experiment of large rotor ERO measuring is implemented after constructing the system.

## 2. Extraction of Electrical Runout

In order to analyze the method of extracting electrical runout, the calculation of impedance of coil is critical. The finite element method is used to compute the impedance in this paper. The physical model of ERO measuring is shown in Fig. 1, because the diameter of rotor is larger than that of eddy current coil, the rotor is simplified by a cubic target. The axis of the solenoid coil of inner radius  $r_1$ , external radius  $r_2$ ,  $N$  turns and height  $h$  is assumed to coincide with the z-axis with the centre of the coil in a cylindrical coordinate system.

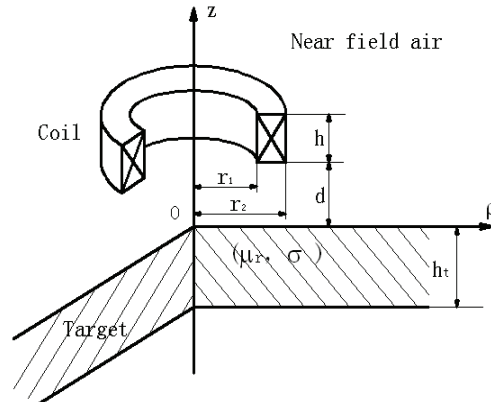


**Fig. 1.** Physical model of eddy current sensor.

The effect of the eddy current in coil, the displacement current, the temperature on resistivity and the velocity of coil can be ignored. According to the Maxwell equation, the eddy current governing equation can be obtained. The magnetic vector potential is found by solving the governing equation using the first boundary conditions. The mapped meshing strategy is adopted on the coil and the target, while the free meshing strategy is adopted in the near field air.

According to Poynting Theorem, after the general energy equation was acquired in light of the first class boundary condition of electromagnetic field and Green's theorem, apply energy minimization. In this way, the final element matrix equation is obtained as

$$[A] = [G]^{-1} [\mathcal{Q}], \quad (1)$$

where  $[A]$  is the unknown magnetic vector potentials at the nodes of the element,  $[G]$  is element matrices formed from the nodes of an element, and  $[Q]$  represents the source term and. Subsequently, the current in coil I can be calculated from  $[A]$  and the excitation voltage U is known. Finally the impedance of coil can be computed as

$$Z = \frac{U \cdot I_r}{I_r^2 + I_i^2} - j \frac{U \cdot I_i}{I_r^2 + I_i^2}, \quad (2)$$

where  $I_r$  and  $I_i$  are the real and imaginary part of coil current respectively,  $U$  is the excitation voltage.

The output of eddy current sensor is in the form of quality factor Q, which is calculated from impedance Z. The calibration curves under different electromagnetic parameters are obtained through finite element model above, which are shown in Fig. 2.

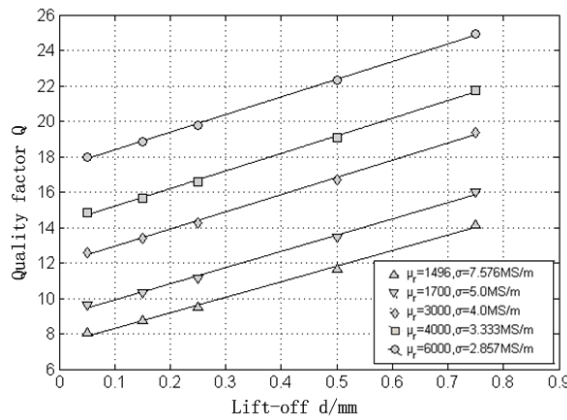


Fig. 2. Calibration curves under different electromagnetic parameters.

The slopes of calibration straight line under different electromagnetic parameters are equal with the maximum relative error 1.6%, which also can be seen in Fig2. Therefore, the slope of calibration line has no relationship with the electromagnetic properties. The output voltage V can be written as

$$V = k \times d + b(\mu, \sigma), \quad (3)$$

where  $k$  is the constant obtained from calibration. Suppose  $d_0$ ,  $\mu_0$ ,  $\sigma_0$  are the parameters of base location of measurement, the corresponding output is

$$V_0 = k \times d_0 + b(\mu_0, \sigma_0) \quad (4)$$

When performing runout measurement for shaft online, the corresponding output is written as

$$V_0 + \Delta V_i = k \times (d_0 + \Delta d_i) + b(\mu_0 + \Delta \mu_i, \sigma_0 + \Delta \sigma_i), \quad (5)$$

where  $\Delta V_i$  is the increment of output. Subtracting (4) from (5), electrical runout  $\Delta e_i$ , which is caused by variation of permeability  $\mu$  and conductivity  $\sigma$ , is obtained as

$$\Delta e_i = \frac{\Delta V_i}{k} - \Delta d_i \quad (6)$$

In this way, as long as variation of lift-off  $\Delta d_i$  is obtained, the electrical runout will be measured easily.

### 3. Measuring System

#### 3.1. Electrical Runout On-Machine Measuring System

According to analysis above, design scheme of electrical runout measuring system based on eddy current sensor and laser triangulation is presented. In the scheme, total indicated runout is measured by eddy current sensor while laser triangulation can only sense change of lift-off, which becomes mechanical runout. At the same time, eddy current sensor is posed in the same plane of measuring cross profile with laser device in order to maintain same measuring profile position. In addition, hall senses the pulse per revolution of rotor for angle phase marking. Fig. 3 shows the system scheme.

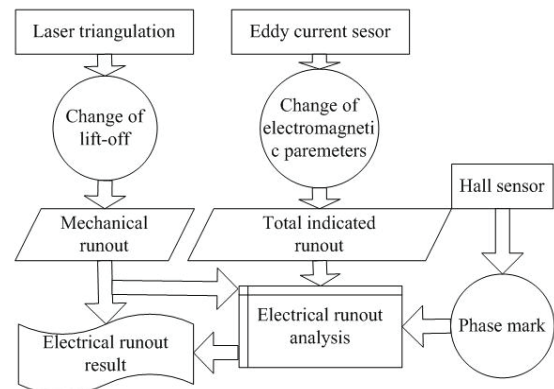


Fig. 3. The scheme frame of measuring system.

#### 3.2. Laser Triangulation Measuring

The principle of laser triangulation is shown in Fig. 4, incident light to the surface of the object to be tested produces scattering light, scattering light is received by the receive parts. Calculation of the displacement is derived by the geometry triangle method as below

$$H = \frac{S}{\frac{S'}{\Delta x} \sin \theta \pm \cos \theta}, \quad (7)$$

where  $H$  is the displacement of the surface of target,  $S$  is the benchmark object distance,  $S'$  is the benchmark image distance,  $\Delta x$  is the displacement of light spot,  $\theta$  is the angle of incoming light beam and optical axis. Sensor receiving components extract and detect displacement changes of light points  $\Delta x$  to calculate the surface displacement of target. Therefore, actual variation of lift-off in eddy current measuring can be detected in this way for electrical runout data calculation.

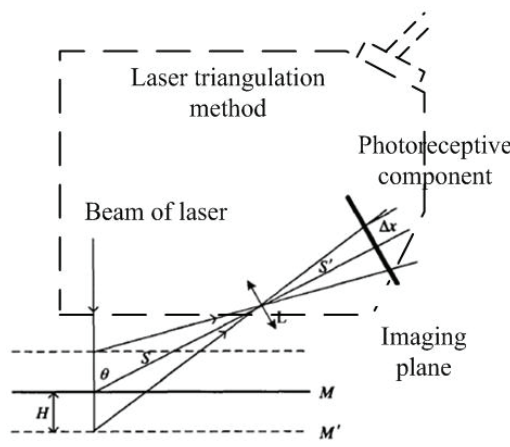


Fig. 4. The principle of triangulation.

Photoelectric receiving component in the system adopts CMOS image conversion sensor, which can be seen in Fig. 5.

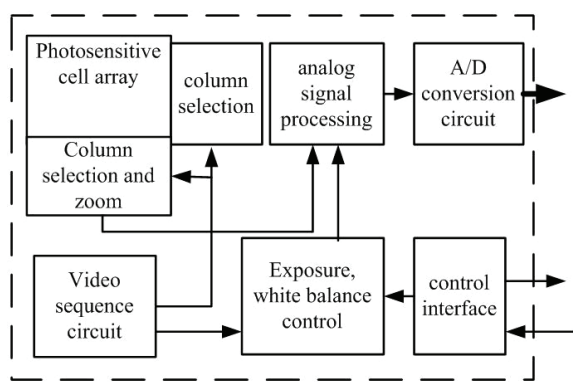


Fig. 5. The component of CMOS.

### 3.3. Elimination of Eccentric Error

Eccentric error is the main error in sensor signal when perform on-machine measuring of rotary rotor. Due to the existence of clamping error, the actual

rotation center  $O$  moves to  $O'$ , so the measured radius becomes  $\overline{AB}$  instead of  $r$ , which can be seen in Fig. 6.

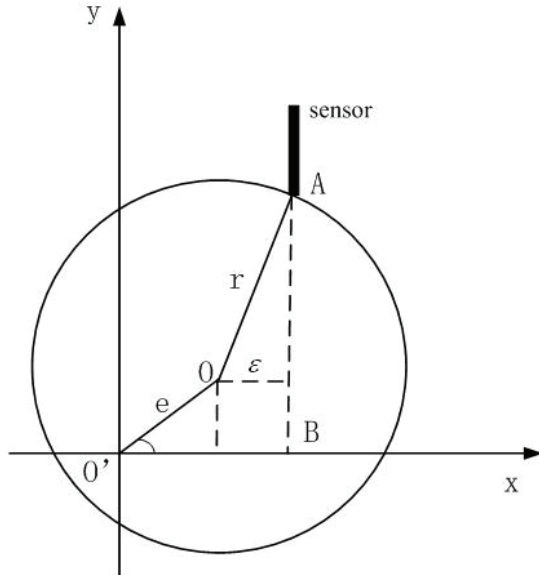


Fig. 6. Eccentric error.

In this system, method of eliminating the first order harmonic is used to separate the eccentric error. Firstly, the first order Fourier harmonic should be computed as

$$\left\{ \begin{array}{l} a = \frac{2}{n} \sum_{i=1}^{n-1} \Delta s(i) \cos\left(\frac{2\pi i}{n}\right) \\ b = \frac{2}{n} \sum_{i=1}^{n-1} \Delta s(i) \sin\left(\frac{2\pi i}{n}\right) \end{array} \right. \quad (8)$$

Then the signal without eccentric error is obtained as below

$$\Delta s'(i) = \Delta s(i) - \left[ a \times \cos\left(\frac{2\pi i}{n}\right) + b \times \sin\left(\frac{2\pi i}{n}\right) \right] \quad (9)$$

### 3.4. Sensor Signal Processing Module

Besides the eccentric error, noise in signal is also need to be eliminated. Discrete Wavelet Transform (DWT) is adopted for multi-resolution sensor signal de composition. The process of de-noising in the system is shown in Fig. 7.

The method of eliminating eccentric error and denoising constitute the main parts of signal data processing module. Fig. 8 shows the flow of data processing.

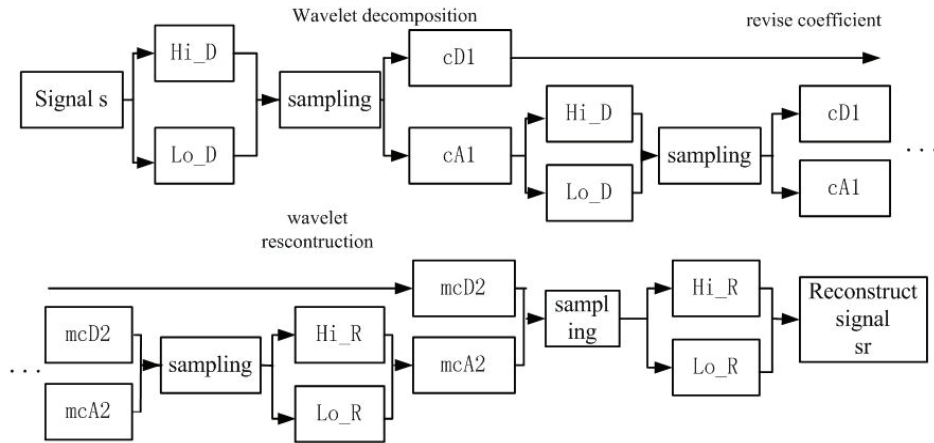


**Fig. 7.** The process of DWT.

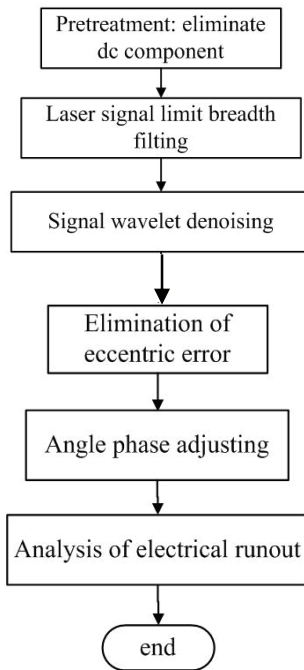


**Fig. 8.** The flow chart of data processing.

#### 4. Experiment on Large Rotors

Verification of developed method is carried out on a large air compressor rotor with eddy current-laser electrical runout measuring system. The experimental system is shown in Fig. 9, eddy current sensor and laser displacement sensor work in the same profile of rotor with a fixed angle, hall sensing a magnetic steel cube, which should be prepared before experiment, for phase marking.

Rotor was mounted in lathe, adjust total runout with a dial indicator under a low speed of revolution in order to limit eccentric error. Then the sensors should be adjusted to appropriate measuring location. When the speed of revolution becomes stable, measuring can be performed. Fig. 10 shows the

experimental photo of test target and measuring procedure.

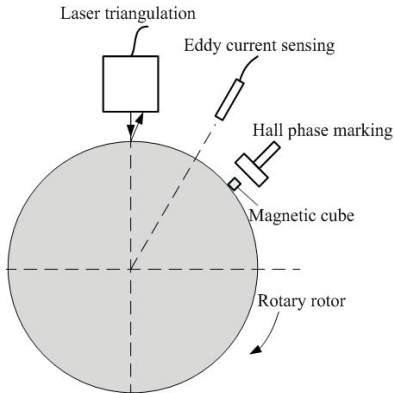


**Fig. 9.** Experimental system sketch.



**Fig. 10.** Experimental photo of target and measuring process.

Experimental measurement was conducted under three revolving speed of lathe, the measuring position is usually on the journal of main shaft (Fig.11). The runout result of measurement is shown in Table 1, runout data per revolution of shaft is drawn in expanded plot and polar plot. Data in polar diagram is added a base circle of 60  $\mu\text{m}$  for better view.

**Table 1.** Experimental runout under different revolving speed.

No.	Speed (r/min)	ERO ( $\mu\text{m}$ )	MRO ( $\mu\text{m}$ )	TIR ( $\mu\text{m}$ )
1.	50	58.57	10.06	53.57
2.	60	62.52	10.19	59.09
3.	80	63.97	9.85	58.06

Electrical runout (ERO),  
Mechanical runout (MRO),  
Total indicated runout (TIR)

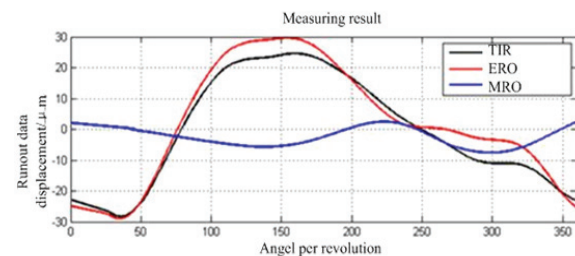
The technical requirement of target rotor is shown in Table 2, which can verify the correctness and accuracy of measuring system. As it seen in result of measured runout, electrical runout is far larger than mechanical runout, which indicates the difficulty of control of electrical runout. Some different low speeds of revolution have no large influence on measuring runout because of the elimination of eccentric error.

**Table 2.** Technical requirement of air compressor rotor.

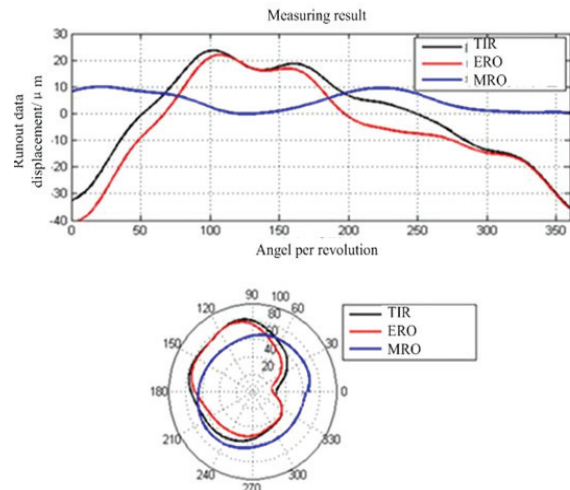
Mark	Diameter of journal	Journal A	Journal B	length of shaft
3SJK1 20	175h6 $(^0_{-0.025})$	Runout 0.01 mm roughness 0.8	Runout 0.01mm roughness 0.8	3750 mm

## 5. Conclusions

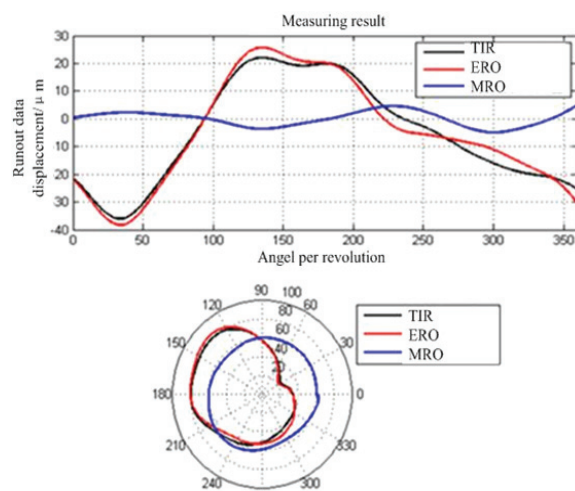
Electrical runout plays an important role in monitoring vibration and reliability of operation. In order to separate electrical runout from change of lift-off in eddy current sensing, finite element model of electrical runout measuring has been established firstly. Method of extracting electrical runout was analyzed based on the impedance influence calculated from FEM. Actual variation of lift-off became critical for electrical runout measuring system. In this way, laser triangulation technique was involved in design of whole system. After design of hardware and software modules, the experiment on large rotor was conducted for verification. It is concluded that the developed system has specially advantage of on-position measuring.



(a) No.1 experimental runout data.



(b) No.2 experimental runout data.



(c) No.3 experimental runout data.

**Fig. 11.** Experimental runout data diagrams.

## Acknowledgements

We would like to acknowledge the support of the National Basic Research Program of P. R. China (973 Program, No. 2011CB706505), the National Natural Science Foundation of the P. R. China (No. 51175466) and Qianjiang Talents Project of Science Technology Department of Zhejiang, China (No. 2011R10016).

## References

- [1]. N. Littrell, Understanding and Mitigating Shaft Runout, *Orbit Magazine*, 2005, 25, pp. 5-17.
- [2]. Mark J. De Block, Barry M. Wood, J. W. McDonnell, Predicting Shaft Proximity Probe Track Runout on API Motors and Generators, *Petroleum and Chemical Industry Technical Conference*, 2007, pp. 1-8.
- [3]. D. H. Biggs, Method for removing electrical runout in machine shafts and apparatus for use with the same, *United States Patent No. 3986380*, 1975.
- [4]. G. Y. Tian, Z. X. Zhao and R. W. Baines, The research of inhomogeneity in eddy current sensors, *Sensors and Actuators A: Physical*, Vol. 69, 1998, pp. 148-151.
- [5]. G Y Tian, A Sophian. Reduction of lift-off effects for pulsed eddy current NDT, *NDT & E International*, 2005, 38, 4, pp. 319-324.
- [6]. Petar B. Petrovic and Zivana Jakovljevic. Dynamic Compensation of Electrical Run-out in Eddy Current Contactless Measurements of Non-Stationary Ferromagnetic Target, *Sensor Letters*, 2009, Vol. 7, pp. 191-202.
- [7]. Yu Yating, Yang Tuo, Du Pingan, A new eddy current displacement measuring instrument independent of sample electromagnetic properties, *NDT&E International*, 48, 2012, pp. 16-22.
- [8]. Y. T. Yu and P. A. Du, Research on the correlation between measured material properties and output of eddy current sensor. in *Proceedings of the IEEE International Conference on Industrial Technology*, Hong Kong, 2005, pp. 428-431.
- [9]. Dodd C. V., Deeds W. E., Luquire J. W., Integral solutions to some eddy current problems, *International Journal of Nondestructive Test*, 1, 1970, pp. 29-90.
- [10]. Cheng C. C., Dodd C. V., Deeds W. E., General analysis of probe coils near stratified conductors. *International Journal of Nondestructive Test*, 3, 1971, pp. 109-130.
- [11]. Dodd C. V., Cheng C. C., Deeds W. E., Induction coils with an arbitrary number of cylindrical conductors, *J. Appl. Phys.*, 45, 1974, pp. 638-647.
- [12]. Theodoros Theodoulidis, Epameinondas Kriezis. Series expansions in eddy current nondestructive evaluation models, *Journal of Materials Processing Technology*, 161, 2005, pp. 343-347.
- [13]. Konrad A., Eddy Current and Modeling, *IEEE Transactions on Magnetics*, Vol.:21, Issue: 5, 1985, pp. 1805-1810.
- [14]. Ida N., Palanisamy R., Lord W., Eddy current probe design using finite element analysis, *Materials Evaluation*, 41, 12, 1983, pp. 1389-1394.
- [15]. Norton S. J., Bowler J. R., Theory of eddy current inversion, *Journal of Applied Physics*, 73, 2, 1993, pp. 501-512.
- [16]. Vyroubal D., Zele D., Experimental optimization of the probe for eddy-current displacement transducer, *IEEE Transactions on Instrumentation and Measurement*, 42, 6, 1993, pp. 995-1000.
- [17]. Kim S. D., Shim J. M., Impedance Analysis and Experimental Study of a Solenoid Eddy Current Sensor to Detect the Cross Section Area of Non Ferromagnetic Stranded Conductors, *J. of Korea Sensor Society*, 6, 2, 1997, pp. 87-94.
- [18]. Tae-Ok Kim, Gil-Seung Lee, Hwa-Young Kim, Jung-Hwan Ahn. Modeling of Eddy Current Sensor using Geometric and Electromagnetic Data, *Journal of Mechanical Science and Technology*, 21, 2007, pp. 465-475.
- [19]. M'hemed Rachek, Mouloud Feliachi. 3-D movement simulation techniques using FE methods: Application to eddy current non-destructive testing, *NDT&E International*, 40, 2007, pp. 35-42.

2013 Copyright ©, International Frequency Sensor Association (IFSA). All rights reserved.  
(<http://www.sensorsportal.com>)

Promoted by IFSA

## Status of the CMOS Image Sensors Industry Report up to 2017

The report describes in detail each application in terms of market size, competitive analysis, technical requirements, technology trends and business drivers.

Order online:

[http://www.sensorsportal.com/HTML/CMOS\\_Image\\_Sensors.htm](http://www.sensorsportal.com/HTML/CMOS_Image_Sensors.htm)